Using lunar boulders to distinguish primary from distant secondary impact craters

Gwendolyn D. Bart[1] and H. J. Melosh[1]

Received 9 January 2007; revised 27 February 2007; accepted 6 March 2007; published 6 April 2007.

[1] A high-resolution study of 18 lunar craters, including both primary and distant secondary craters, shows that the secondary craters produce larger ejecta fragments at a given crater size than do the primary craters. The maximum boulder diameter (B) increases with crater size (D) according to the power law $B = KD^{2/3}$; for primary craters, when B and D are in meters, K is 0.29, whereas for secondary craters, we find that K is 0.46 (60% larger). Next we show that impact fracture theory predicts that secondary craters, because of their lower impact velocity, will produce larger ejecta fragments than primary craters. This result provides an opportunity for distinguishing between primary and secondary craters in high resolution planetary images. The ability to identify distant secondary craters will help constrain primary production rates of small craters and improve surface age determination of small areas based on small crater counts. **Citation:** Bart, G. D., and H. J. Melosh (2007), Using lunar boulders to distinguish primary from distant secondary impact craters, *Geophys. Res. Lett.*, *34*, L07203, doi:10.1029/2007GL029306.

1. Introduction

[2] Planetary surface ages can help distinguish sequences of geologic events, revealing clues to a planet's evolution. Although radiometric dating is the most accurate and reliable way to date a rock, the only body besides Earth for which we have samples from known locations is the Moon. To determine ages of unsampled planetary surfaces, counts of craters on the surface provide a relative age; more heavily cratered surfaces are generally older [*Shoemaker et al.*, 1963]. The ages of lunar surfaces at the *Apollo* landing sites were measured both ways, providing a single-point calibration of the crater density dating method.

[3] The crater density dating method is reliable for large craters over broad surface areas. However, spacecraft are beginning to return images at meter scale or better resolution, permitting counts of smaller craters. Can these small craters be used for determining the age of a surface? Some small craters are secondary craters, meaning that the impactor was launched as ejecta from another crater, rather than falling from interplanetary space. Secondary craters near their primary crater were formed by impact velocities <1 km/s [*Melosh*, 1989] and hence can be distinguished by a characteristic morphology, including irregular shape, shallow depth, location in crater chains, and a herringbone ejecta pattern [*Shoemaker*, 1962; *Oberbeck and Morrison*, 1973]. Distant secondary craters, however, are launched at higher velocities, and are morphologically similar to small primary craters. How many of the small craters at a given location are secondary craters? Which ones are the secondary craters? The answer is crucial for reliable age determination.

[4] If most of the small craters are primaries, as some have assumed [*Neukum and Ivanov*, 1994], their production is random in time and space, and hence they can be used to determine surface ages. However, both old lunar results [*Shoemaker*, 1965] and recent results from Europa [*Bierhaus et al.*, 2001, 2005] and Mars [*McEwen et al.*, 2005; *McEwen and Bierhaus*, 2006] indicate that the small crater population is dominated by secondary craters. Because secondary craters are clustered in time and space, they do not provide a reliable chronometer.

[5] While pursuing a better understanding of impact crater ejecta distributions, we discovered a quantifiable difference between the ejecta fragment sizes of primary and distant secondary craters. This ejecta size difference provides an opportunity for distinguishing between primary and secondary craters in high resolution planetary images. Identification of distant secondary craters will help constrain primary production rates of small craters and improve surface age determination of small areas based on small crater counts.

2. Identification of Distant Secondary Craters

[6] Distant secondary craters are difficult to identify because their impactors have higher velocities than the impactors that create secondary craters near the primary. As a result, the distant secondary craters have morphologies similar to those of primary craters. The first distant secondary craters unambiguously identified are those from a 25 km primary crater named Pwyll located on Jupiter's moon Europa [*Bierhaus et al.*, 2001]. Because Europa's surface is so young, relatively few primary craters exist on its surface. Small craters (<1 km) are spatially associated with the crater rays, indicating that they are secondary craters. On Mars, distant secondary craters of Zunil are identified by a distinctive thermal inertia signature of the secondary crater's ejecta, as well as by association of the secondary crater with Zunil's rays [*McEwen et al.*, 2005].

[7] We think it likely that several lunar mare craters associated with a ray from the crater Burg are distant secondary craters. Burg is a 39.1 km diameter crater with distinct rays extending across Mare Serenitatis [*Grier et al.*, 2001]. Several of these lunar craters are likely distant secondary craters because of their association with the Burg ray, their apparent similar age, and their proximity to one another. However, due to the abundance of lunar primary craters, and the poor quality, resolution, and lighting of the

[1]Department of Planetary Science, University of Arizona, Tucson, Arizona, USA.

0094-8276/07/2007GL029306$05.00

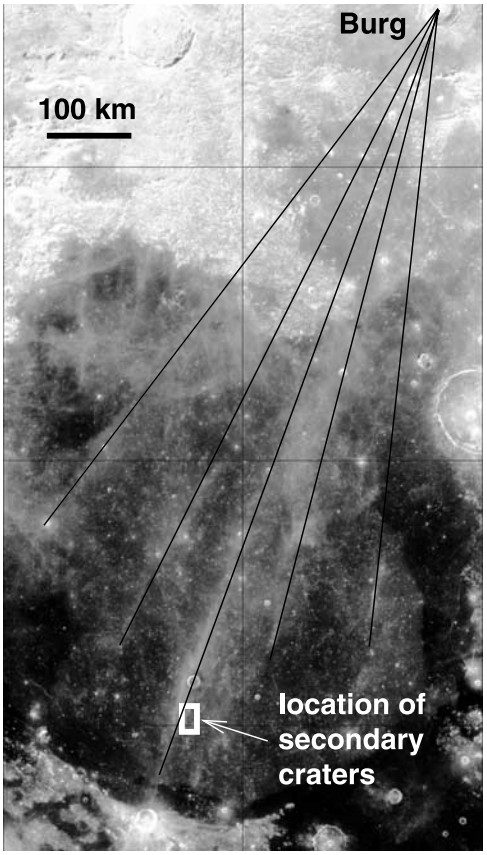

Figure 1. A *Clementine* basemap image shows the rays from the crater Burg extending across Mare Serenitatis. The location of the Burg ray craters is indicated. Several of these craters are probably distant secondary craters. North is up.

photographs, it is difficult to verify that they are secondary craters. Figure 1 shows the location of these craters with respect to Burg.

[8] To be secondary craters of Burg, the ejection velocity of the fragments that formed them must be less than the Moon's escape velocity. That ejection velocity is computed assuming a spherical Moon, and is given by

$$v_{ej} = \sqrt{\frac{gR_p \tan\phi}{\sin\theta\cos\theta + \cos^2\theta\tan\phi}} \quad (1)$$

where v_{ej} is the ejection velocity, g is the surface gravity (1.62 m/s^2 for the Moon), R_p is the body's radius (1737 km for the Moon), ϕ, the half angular distance of travel is $R/2R_p$, and R is the distance of the secondary crater from its primary (in this case, 890 km) [*Vickery*, 1986]. We assume an ejection angle, θ, of 45°; this value is not critical since the equation is not a strong function of θ for $\theta = 45° \pm 15°$. This equation gives an ejection velocity of 1080 m/s for the fragments that formed Burg secondary craters in this area. This value is comfortably less than the lunar escape velocity of 2380 m/s.

3. Method

[9] We compare six of the Burg ray craters with six additional mare craters and six highlands craters. The small number of craters studied results from the paucity of high-resolution photographs of the lunar surface. The craters are observed in high resolution (1–4 m) photographs from *Lunar Orbiter III* and *V* and *Apollo 17*. The *Lunar Orbiter* and *Apollo* photographs were taken on photographic film in 1967 and 1972, respectively. Because photographic prints do not have a meaningful m/pixel resolution value, the resolution is given as the extent of the smallest feature observed in the image. No more recent spacecraft has returned higher resolution images of the Moon. The *Lunar Reconnaissance Orbiter Camera* will return high quality, 0.5 m/pixel images (http://lroc.sese.asu.edu/specifications.html) from the Moon after it launches in 2008, enabling a more through study of ejected lunar boulders.

[10] We used the computer program *ImageJ* (W. S. Rasband, ImageJ, U.S. National Institutes of Health, Bethesda, Maryland, 1997–2006, available at http://rsb.info.nih.gov/ij) to measure the diameter of every boulder in the image associated with each crater. Boulders were visible from the rim out to about 4–10 crater radii. In most cases boulders stopped being visible before the edge of the image was reached. Boulders were identified as bright pixel(s) on the sunward side of dark pixel(s) (shadows). We made the measurement perpendicular to the sun direction to eliminate uncertainty of the extent of the boulder into its shadow. We determined the crater diameters by fitting several 20–30 sided polygons to the rim of the crater, finding the center of those polygons with *ImageJ*, and taking the average of the results. This average polygon technique reduces random measurement errors, but cannot eliminate possible systematic error based on selection of rim location.

Table 1. Photograph Number[a], Diameter of the Largest Boulder Around Each Crater, Mean Diameter of the Five Largest Boulders, Crater Diameter, and the Latitude and Longitude of Each Photograph[b]

Photo Number	Largest Boulder (m)	Mean of 5 Largest (m)	Crater Diam (m)	Photo Latitude	Photo Longitude
		Burg Ray Craters			
Ap17-2345(a)	57	13	1060	20°N	18°E
Ap17-2345(b)	44	32	1300	20°N	18°E
Ap17-2345(e)	31	13	1415	20°N	18°E
Ap17-2345(f)	41	13	730	20°N	18°E
Ap17-2345(g)	44	9	674	20°N	18°E
Ap17-2345(i)	47	9	591	20°N	18°E
		Highlands Craters			
V-63-H2	69	10	4000	1°S	33°E
V-82-M	410	310	27400	3°N	18°E
V-152-H2	16	6	506	10°N	20°W
V-153-H2	54	7	881	10°N	20°W
V-167-H2(b)	17	6	452	13°N	31°W
V-167-H3	23	8	690	13°N	31°W
		Other Mare Craters			
III-185-H3	14	5	290	2°S	44°W
III-186-H2	17	5	678	2°S	44°W
III-186-H3	16	5	229	2°S	44°W
III-189-H2	21	6	537	2°S	44°W
V-199-M	360	330	41200	23°N	47°W
V-211-H3	17	4	520	14°N	56°W

[a]Photo numbers III and V indicate *Lunar Orbiter III* and *V* photographs; Ap17-2345 indicates *Apollo 17* panoramic camera photograph number 2345. Letters designate individual craters in a photograph.

[b]Photograph locations are reported because the specific locations of the craters themselves cannot be determined from the photographic prints.

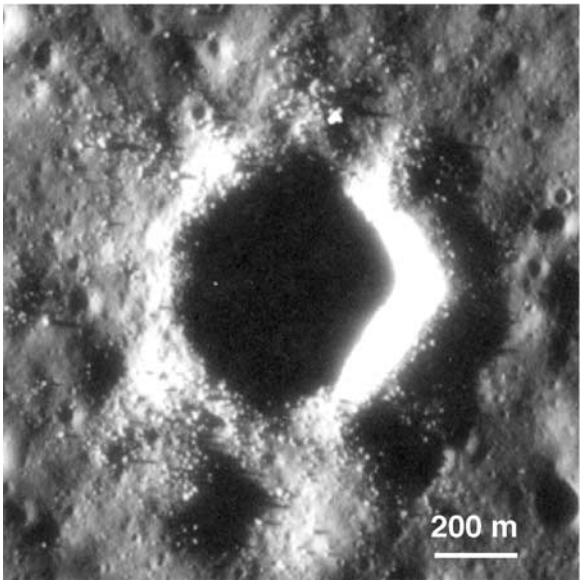

Figure 2. A crater in *Apollo 17* panoramic camera photograph number 2345 is surrounded by boulders. This crater is likely a distant secondary crater of Burg, a 39.1 km diameter crater on the northeast edge of Mare Serenitatis. The sun shines from the left in this photograph; the right wall of the crater is illuminated, and boulder shadows fall to the right.

[11] The diameter of the largest boulder ejected from each crater is given in Table 1. To reduce the stochastic variations we expect in the maximum boulder size, we calculate the mean of the five largest boulders about each crater, listed in the next column. Table 1 also reports each crater's diameter, the photograph numbers where each crater was observed, and the center latitude and longitude of each image. (It is not possible to determine the longitude and latitude of the individual craters from the photographic prints, and more recent lunar maps have too low a resolution to identify these craters.) Figure 2 is an image of one of the Burg secondary craters and its boulders.

4. Results

[12] For each of the 18 craters, we plot the mean diameter of the five largest boulders about each crater vs. crater diameter (Figure 3). The data show an increase in boulder diameter with crater diameter. *Moore* [1971] empirically determined that the maximum diameter, B, of a boulder ejected from an impact or explosion crater increases regularly with crater diameter, D, according to the equation

$$B = KD^{2/3}, \tag{2}$$

where K ranges from 0.11 to 0.32 when B and D are in meters. The equation holds for craters as large as Tycho and Aristarchus on the Moon, as well as for explosion craters, and for centimeter size experimental impact craters.

[13] Our lunar data also follow this equation, and two lines with slope 2/3 have been plotted. The lower line, $y = 0.29x^{2/3}$, is the best fit line through the "other" (not Burg ray) mare craters (open squares), and the K value falls well within the expected K values published by *Moore* [1971]. Two Burg ray craters (open circles) also plot along this line. The upper line, $y = 0.46\ x^{2/3}$, plots through the remainder of the Burg ray craters. Its K (0.46) is 44% greater than the maximum K (0.32) given by *Moore* [1971], and 59% greater than the K (0.29) that fits all the other mare craters. These Burg ray craters with elevated K values are likely secondary craters. Impact crater theory, described in section 5, predicts that craters formed by impactors with lower velocity (e.g., secondary craters) will have larger boulders than craters formed by higher velocity impactors (primary craters).

[14] The highlands craters (closed triangles), with one exception, plot along the lower (primary crater) line with the "other" mare craters. This result indicates that terrain type is unimportant in determining the maximum block sizes ejected by a crater. We had expected that craters on different terrain, which may be underlain by rocks of very different intrinsic strength, would produce different block sizes, with weaker substrate fracturing more easily and producing smaller boulders. Nevertheless, this idea is not supported by our data. There is one highlands crater that plots along the higher line; it may be another distant secondary crater. Unfortunately, we have not observed any supporting evidence for that claim in the photograph of that crater.

5. Boulder Size and Impact Velocity

[15] The size of boulders ejected from an impact crater depends on the size of the crater, the strength and condition of the substrate rock (whether it is initially fractured or jointed) and the impact velocity. Other factors being equal, the size of the ejected boulders is inversely correlated with impact velocity: craters produced by lower velocity impacts

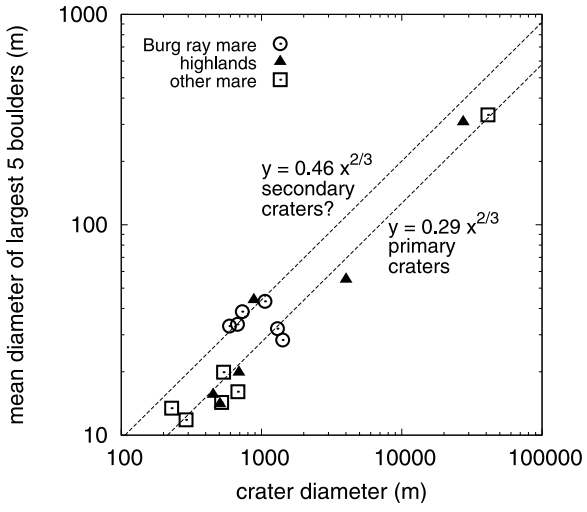

Figure 3. Plot of the mean diameter of the five largest boulders around each crater vs. that crater's diameter. The boulder sizes increase with increasing crater size along a power law with exponent 2/3, as previously found by *Moore* [1971]. The lower line fits through most of the data, and has an intercept (K value, equation (2)) that falls within the range of the primary craters studied by *Moore* [1971]. Several of the Burg ray craters fall along a line with a 60% greater K value. These craters are likely distant secondary craters.

should produce larger boulders. The complete explanation of this relation is quite complex. Fragment sizes in rapidly crushed rock depend on both the size of the stress load as well as the loading rate [*Collins et al.*, 2004; *Melosh et al.*, 1992]. However, for a given final crater size, lower velocity impacts produce both a lower peak stress as well as a lower loading rate, both of which favor larger fragments. The peak stress is readily estimated from the second Hugoniot equation, in which the longitudinal stress in a planar shock wave is the product of initial density ρ_0, particle velocity u_p, and shock velocity U. Using the linear particle-velocity shock velocity approximation in the planar impact approximation [*Melosh*, 1989, p. 39, 54ff., and Appendix II], the peak shock pressure is given by

$$P_{\max} = \frac{\rho_0 v_i}{2}\left(C + \frac{S v_i}{2}\right), \tag{3}$$

where v_i is the impact velocity, and C and S are equation of state parameters. We assume that the projectile and target are identical in composition, a reasonable assumption since the result is fairly insensitive to factors of a few. Using the equation of state parameters for basalt ($\rho_0 = 2860$ kg/m^3, $C = 2.60$ km/s, and $S = 1.62$) [*Melosh*, 1989, Appendix II], the peak shock pressure is 12 GPa for an impact at 2 km/sec, near the maximum impact velocity for secondary craters on the Moon, given its escape velocity, and 500 GPa for an impact of 19.2 km/sec, the average lunar primary impactor velocity [*Stuart and Binzel*, 2004]. The shock pressure for a primary impact is thus more than 40 times larger than that for a secondary. This does not mean that boulders ejected from secondary craters of a given size are 40 times larger than those from primary impact craters of the same size, because the crater size also increases with increasing impact velocity, but it does indicate that, in general, the shock pressure is lower in craters produced by secondary impacts.

[16] Boulder (fragment) size is largely a function of the stress gradient (as well as strain rate) in the target rock. Thus, for a given size crater, higher shock pressure (caused by higher impact velocity) generates larger stress gradients (that is, larger stress per unit distance), hence smaller spacing between fractures and thus smaller fragments for a given crater size, as we have discovered observationally.

6. Discussion

[17] A practical technique for distinguishing distant secondary craters from primary craters will be a valuable tool for the planetary science surfaces community. The data and theory presented in this paper suggest that a crater may be a distant secondary if the K value (equation (2)) of the mean of the five largest boulders around a crater exceeds the normal range of K values for primary craters. Nevertheless, until more data substantiates this expectation, caution should be exercised in implementing this technique.

[18] An important consideration is whether this technique will be applicable to Mars as well as the Moon. Because of the vast number of high resolution images that are being returned from Mars by the *Mars Reconnaissance Orbiter* HiRISE camera [*McEwen et al.*, 2002], it would be particularly valuable to apply this method to that planet. However, this method may not be quite as effective on Mars. Mars has a higher escape velocity than the Moon (5 km/s vs. 2.4 km/s), but a lower average primary impact velocity than the Moon(10 km/s [*Ivanov*, 2001] vs. 19.2 km/s [*Stuart and Binzel*, 2004]). Thus the martian primary impact velocity is only two times greater than the secondary impact velocity, whereas the lunar primary impact velocity is ten times greater than the secondary impact velocity. These values correlate to peak shock pressures (equation (3)) for primary impacts on Mars three times larger than for secondary impacts, whereas on the Moon, the peak shock pressures for primary craters are 40 times greater than for secondary impacts. A study of the boulder sizes of, for example, the secondary craters of Zunil [*McEwen et al.*, 2005] on Mars, compared with other small craters not obviously associated with a primary crater is needed to determine whether this difference is sufficient for identification of distant secondary craters on Mars.

7. Conclusion

[19] The larger K values (equation (2)) associated with several of the Burg ray craters, in conjunction with the predictions from impact crater theory, suggest a distinction between primary craters (higher velocity impacts) and secondary craters (lower velocity impacts). This method requires high resolution images to resolve the meter-size boulders ejected from craters in the hundred-meter crater size range; the expected return of such images in the next few years from the *Mars Reconnaissance Orbiter* HiRISE camera and the *Lunar Reconnaissance Orbiter Camera* will enable further validation of this method. The discovery of this technique for distinguishing primary and distant secondary impact craters may rescue attempts to date very young planetary surfaces, even in the face of heavy contamination by secondary craters.

[20] **Acknowledgments.** We would like to thank Beau Bierhaus and an anonymous reviewer for comments which helped us improve this paper. Thanks also to Robert Strom for fruitful discussions about ejected boulders and 1960s spacecraft photographs. This work was supported by the Lunar and Planetary Laboratory, University of Arizona, and NASA PGG grant NNG05GK40G.

References

Bierhaus, E. B., C. R. Chapman, W. J. Merline, S. M. Brooks, and E. Asphaug (2001), Pwyll secondaries and other small craters on Europa, *Icarus*, *153*, 264–276, doi:10.1006/icar.2001.6690.

Bierhaus, E. B., C. R. Chapman, and W. J. Merline (2005), Secondary craters on Europa and implications for cratered surfaces, *Nature*, *437*, 1125–1127, doi:10.1038/nature04069.

Collins, G. S., H. J. Melosh, and B. A. Ivanov (2004), Modeling damage and deformation in impact simulations, *Meteorit. Planet. Sci.*, *39*, 217–231.

Grier, J. A., A. S. McEwen, P. G. Lucey, M. Milazzo, and R. G. Strom (2001), Optical maturity of ejecta from large rayed lunar craters, *J. Geophys. Res.*, *106*(E12), 32,847–32,862.

Ivanov, B. A. (2001), Mars/Moon cratering rate ratio estimates, *Space Sci. Rev.*, *96*, 87–104, doi:10.1023/A:1011941121102.

McEwen, A. S., and E. B. Bierhaus (2006), The importance of secondary cratering to age constraints on planetary surfaces, *Annu. Rev. Earth Planet. Sci.*, *34*, 535–567, doi:10.1146/annurev.earth.34.031405.125018.

McEwen, A. S., et al. (2002), HiRISE: The High Resolution Imaging Science Experiment for Mars Reconnaissance Orbiter, *Lunar Planet. Sci.*, *XXXIII*, abstract 1163.

McEwen, A. S., B. S. Preblich, E. P. Turtle, N. A. Artemieva, M. P. Golombek, M. Hurst, R. L. Kirk, D. M. Burr, and P. R. Christensen (2005), The rayed crater Zunil and interpretations of small impact craters on Mars, *Icarus*, *176*, 351–381, doi:10.1016/j.icarus.2005.02.009.

Melosh, H. J. (1989), *Impact Cratering: A Geologic Process*, Oxford Univ. Press, New York.

Melosh, H. J., E. V. Ryan, and E. Asphaug (1992), Dynamic fragmentation in impacts: Hydrocode simulation of laboratory impacts, *J. Geophys. Res.*, *97*, 14,735–14,759.

Moore, H. J. (1971), Large blocks around lunar craters, in *Analysis of Apollo 10 Photography and Visual Observations*, *NASA Spec. Publ. SP-232*, 26–27.

Neukum, G., and B. A. Ivanov (1994), Crater size distributions and impact probabilities on Earth from lunar, terrestrial-planet, and asteroid cratering data, in *Hazards Due to Comets and Asteroids*, *Space Sci. Ser.*, edited by T. Gehrels, M. S. Matthews, and A. M. Schumann, pp. 359–416, Univ. of Ariz. Press, Tucson.

Oberbeck, V. R., and R. H. Morrison (1973), On the formation of the lunar herringbone pattern, *Proc. Lunar Planet. Sci. Conf. 4th*, 107–123.

Shoemaker, E. M. (1962), Interpretation of lunar craters, in *Physics and Astronomy of the Moon*, edited by Z. Kopal, pp. 283–360, Elsevier, New York.

Shoemaker, E. M. (1965), Preliminary analysis of the fine structure of the lunar surface in Mare Cognitum, in *The Nature of the Lunar Surface*, edited by W. N. Hess, D. H. Menzel, and J. A. O'Keefe, pp. 23–77, Johns Hopkins Univ. Press, Baltimore, Md.

Shoemaker, E. M., R. J. Hackman, and R. E. Eggleton (1963), Interplanetary correlation of geologic time, *Adv. Astronaut. Sci.*, *8*, 70–89.

Stuart, J. S., and R. P. Binzel (2004), Bias-corrected population, size distribution, and impact hazard for the near-Earth objects, *Icarus*, *170*, 295–311, doi:10.1016/j.icarus.2004.03.018.

Vickery, A. M. (1986), Size-velocity distribution of large ejecta fragments, *Icarus*, *67*, 224–236.

G. D. Bart and H. J. Melosh, Department of Planetary Science, University of Arizona, Tucson, AZ 85721, USA. (gwenbart@LPL.arizona.edu)